

Northumbria Research Link

Citation: Iacocca, Ezio and Hoefler, Mark A. (2019) Perspectives on spin hydrodynamics in ferromagnetic materials. Physics Letters A, 383 (28): 125858. ISSN 0375-9601

Published by: UNSPECIFIED

URL:

This version was downloaded from Northumbria Research Link: <http://northumbria-test.eprints-hosting.org/id/eprint/52678/>

Northumbria University has developed Northumbria Research Link (NRL) to enable users to access the University's research output. Copyright © and moral rights for items on NRL are retained by the individual author(s) and/or other copyright owners. Single copies of full items can be reproduced, displayed or performed, and given to third parties in any format or medium for personal research or study, educational, or not-for-profit purposes without prior permission or charge, provided the authors, title and full bibliographic details are given, as well as a hyperlink and/or URL to the original metadata page. The content must not be changed in any way. Full items must not be sold commercially in any format or medium without formal permission of the copyright holder. The full policy is available online: <http://nrl.northumbria.ac.uk/policies.html>

This document may differ from the final, published version of the research and has been made available online in accordance with publisher policies. To read and/or cite from the published version of the research, please visit the publisher's website (a subscription may be required.)



Northumbria
University
NEWCASTLE



UniversityLibrary

Perspectives on spin hydrodynamics in ferromagnetic materials

Ezio Iacocca^a, Mark A. Hofer^a

^a*Department of Applied Mathematics, University of Colorado, Boulder, Colorado 80309-0526, USA*

Abstract

The field of spin hydrodynamics aims to describe magnetization dynamics from a fluid perspective. For ferromagnetic materials, there is an exact mapping between the Landau-Lifshitz equation and a set of dispersive hydrodynamic equations. This analogy provides ample opportunities to explore novel magnetization dynamics and magnetization states that can lead to applications relying entirely upon magnetic materials, for example, long-distance transport of information. This article provides an overview of the theoretical foundations of spin hydrodynamics and their physical interpretation in the context of spin transport. We discuss other proposed applications for spin hydrodynamics as well as our view on challenges and future research directions.

1. Introduction

A new paradigm for magnetic-based technologies is to expand the functionality and energy efficiency of spintronic devices [1] by utilizing spin currents [2, 3]. Spin currents describe the transport of angular momentum by particles or quasi-particles. The quintessential spin-carrying particle is the electron. Spin currents carried by electrons can be generated in nonmagnetic [4, 5] and magnetic [6, 7] metals, but are necessarily accompanied by a net charge current. This charge current incurs energy dissipation via Joule heating that limits the energy efficiency of charge-to-spin interconversion. Despite this shortcoming, spin currents hold promise for current-controlled magnetization dynamics and their applications [3]

Spin waves are fundamental magnetic excitations that also carry spin current as quantum-mechanical quasi-particles known as magnons [8]. In the context of spin transport, the spin transfer torque [9, 10]

Email address: ezio.iacocca@colorado.edu (Ezio Iacocca)

and the spin pumping [11, 12] effects provide an interconversion mechanism between angular momentum and charge currents at a magnet / metal interface. A technological advantage of spin waves is that their existence is independent of the conduction properties of the material. This implies that energy dissipation associated to conduction electrons is minimized. However, spin waves are subject to scattering processes that ultimately limit their coherence [13].

The amplitude of a spin wave decays exponentially with a decay length equal to $v_g/(2\omega\alpha)$ [14], where v_g , ω , and α are, respectively, the spin wave group velocity, angular frequency, and the magnetic Gilbert damping parameter [15]. To maximize the decay length, low damping materials such as Permalloy ($\text{Ni}_{80}\text{Fe}_{20}$) and YIG have been regularly used for research on all-magnetic logic and computation [16]. Decay lengths on the order of micrometers have been obtained in these materials [14, 17, 18]. Recently, long-distance spin transport in amorphous Yttrium-Iron ferrite [19] and antiferromagnetic haematite [20] was measured experimentally. However, the finite Gilbert damping parameter and the concomitant exponential decay of spin waves remains a presently insurmountable limitation for magnon-based technologies.

To beat exponential decay, other forms of spin transport must be explored. Spin hydrodynamics offers such an alternative via the stabilization of noncollinear, large-amplitude magnetization states in magnetic materials with dominant easy-plane anisotropy. Because of its potential impact on technologies that rely on the control of spin, the field of spin hydrodynamics has experienced a rapid growth over the last five years, including recent experimental evidence [21, 22] for hydrodynamic-like spin transport.

In light of multiple recent theoretical developments, we provide in this article an overview of the theoretical studies on spin hydrodynamics in ferromagnetic materials. We review the dispersive hydrodynamic formulation of magnetization dynamics and its physical interpretation. We also discuss the theoretical predictions pertaining to the properties of ideal and current-induced spin hydrodynamic states in the context of long-distance spin transport. Finally, we discuss challenges and possible research directions.

2. Fluid interpretation of magnetization dynamics

2.1. Micromagnetic equations of motion

The dynamics of the ferromagnetic space- and time-dependent magnetization vector \mathbf{M} can be described by the Landau-Lifshitz (LL) equation [23]

$$\partial_t \mathbf{M} = -\gamma \mu_0 \left[\mathbf{M} \times \mathbf{H}_{\text{eff}} + \frac{\alpha}{M_s} \mathbf{M} \times (\mathbf{M} \times \mathbf{H}_{\text{eff}}) \right], \quad (1)$$

where $M_s = |\mathbf{M}|$ is the saturation magnetization, γ is the gyromagnetic ratio, μ_0 is the vacuum permeability, and α can be utilized in the LL form of Eq. (1) when $\alpha \ll 1$. \mathbf{H}_{eff} is an effective field that models the relevant physics acting on the magnetic material. For simplicity, we primarily consider thin film materials with dominant uniaxial symmetry so that the effective field includes an external field, uniaxial anisotropy, and exchange,

$$\mathbf{H}_{\text{eff}} = \underbrace{\mathbf{H}_0}_{\text{external field}} - \underbrace{(1 - h_k)(\mathbf{M} \cdot \hat{\mathbf{z}})\hat{\mathbf{z}}}_{\text{uniaxial anisotropy}} + \underbrace{\lambda_{\text{ex}}^2 \Delta \mathbf{M}}_{\text{exchange}}. \quad (2)$$

Here, $h_k = H_k/M_s$ is a perpendicular anisotropy field that can arise, e.g., from surface effects in multilayers [24]; the $(-\mathbf{M} \cdot \hat{\mathbf{z}})\hat{\mathbf{z}}$ term corresponds to the local demagnetizing field in a thin film with a uniform magnetization in the perpendicular-to-plane direction $\hat{\mathbf{z}}$; and $\lambda_{\text{ex}} = \sqrt{2A/(\mu_0 M_s^2)}$ is the exchange length with A being the exchange constant.

We can identify two fundamentally distinct hydrodynamic regimes by introducing the quantity $\sigma = \text{sgn}(1 - h_k)$. The sign $\sigma = 1$ represents materials with easy-plane anisotropy, e.g. Py, which we will show to be hydrodynamically *stable*, and $\sigma = -1$ represents materials with perpendicular magnetic anisotropy, e.g., Co/Ni multilayers, which are hydrodynamically *unstable*. The case $\sigma = 0$, i.e., $h_k = 1$, represents isotropic ferromagnets that are not considered here.

To simplify notation, it is convenient to work with the dimensionless LL equation [25]

$$\partial_t \mathbf{m} = -\mathbf{m} \times \mathbf{h}_{\text{eff}} - \alpha \mathbf{m} \times (\mathbf{m} \times \mathbf{h}_{\text{eff}}), \quad (3a)$$

$$\mathbf{h}_{\text{eff}} = h_0 \hat{\mathbf{z}} - \sigma (\mathbf{m} \cdot \hat{\mathbf{z}})\hat{\mathbf{z}} + \Delta \mathbf{m}, \quad (3b)$$

where $\mathbf{m} = \mathbf{M}/M_s$, fields are scaled by $|1 - h_k|M_s$, space is scaled by $\sqrt{|1 - h_k|}\lambda_{\text{ex}}^{-1}$, and time is scaled by $\gamma \mu_0 M_s |1 - h_k|$.

2.2. Hydrodynamic transformation

The fluid interpretation of the LL equation, Eq. (1), was first proposed by Halperin and Hohenberg [26] in the context of spin wave dispersion. For an easy-plane ferromagnet, a canonical transformation between the magnetization vector and a spin density and fluid velocity is [27]

$$n = m_z, \quad (4a)$$

$$\mathbf{u} = -\nabla\Phi = -\nabla[\arctan(m_y/m_x)], \quad (4b)$$

where the normalized magnetization is $\mathbf{m} = (m_x, m_y, m_z)$, n is the longitudinal spin density, and \mathbf{u} is the fluid velocity equal to the negative gradient of the azimuthal angle Φ .

The spin density defined in Eq. (4a) is bounded by the magnetization vector magnitude, $|n| \leq 1$. In contrast with typical fluids, the spin density is also signed. When the density is either $+1$ or -1 , the azimuthal angle Φ , hence the fluid velocity \mathbf{u} , is not defined. This implies that $n = \pm 1$ corresponds to vacuum [25]. In contrast, $n = 0$ corresponds to density saturation.

The fluid velocity given in Eq. (4b) is irrotational, i.e., $\nabla \times \mathbf{u} = \nabla \times (-\nabla\Phi) = 0$ in non-vacuum regions where Φ is defined. A direct consequence is that vortices can only appear in a quantized manner via a density vacuum point [28]. Theoretically, the fluid velocity is unbounded. However, because the transformation (4) is applied to the LL equation in a micromagnetic approximation, the concept of a fluid velocity is valid insofar as $|\mathbf{u}| \lesssim |1 - h_k|^{-1/2}$, corresponding to physical length scales larger than or on the order of λ_{ex} .

To better illustrate the physical meaning of the fluid velocity, it is insightful to consider the simple case of a spin supercurrent [29] where $n = 0$ and the azimuthal angle is a linear function of space, e.g., $\Phi = -\bar{u}x$. This describes a spiraling, static magnetization texture with a constant phase difference between neighboring magnetization vectors similar to a spin-density wave (SDW) [30] as depicted in Fig. 1. The fluid velocity is simply equivalent to the SDW wavenumber. Note that we have not considered any time dependence. As such, the fluid velocity can be nonzero even for a static texture such as a SDW [25, 31]. We stress that SDWs are defined for any $n = \bar{n}$ that can be stabilized by an external field $\mathbf{h}_0 = -\bar{n}\hat{\mathbf{z}}$ for $|\bar{n}| < 1$ [31].

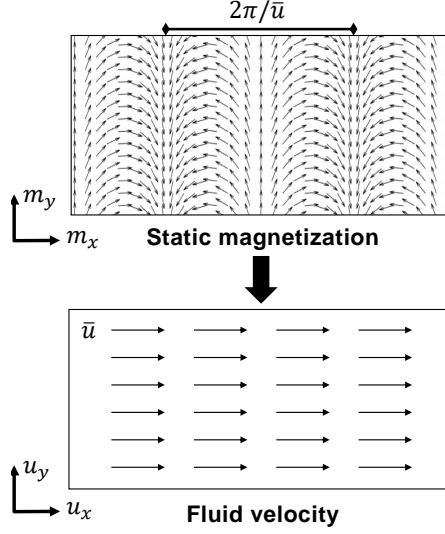


Figure 1: Spin-density wave exhibiting a static, spiraling magnetization texture for the in-plane magnetization, m_x and m_y . The equivalent fluid representation is a uniform flow \mathbf{u} . The fluid velocity is equivalent to the spin-density wave wavevector, as depicted in the top panel.

3. Noncollinear magnetization states

3.1. Dispersive hydrodynamic formulation

Performing the transformation (4) on the dimensionless LL equation (3a) and (3b) yields a set of dispersive hydrodynamic (DH) equations [25, 31]

$$\frac{\partial n}{\partial t} = \underbrace{\nabla \cdot [(1-n^2)\mathbf{u}]}_{\text{spin density flux}} + \underbrace{\alpha(1-n^2)}_{\text{spin relaxation}} \frac{\partial \Phi}{\partial t}, \quad (5a)$$

$$\begin{aligned} \frac{\partial \mathbf{u}}{\partial t} = & \underbrace{\nabla [(\sigma - |\mathbf{u}|^2)n]}_{\text{velocity flux}} - \underbrace{\nabla \left[\frac{1}{\sqrt{1-n^2}} \nabla \cdot \left(\frac{\nabla n}{\sqrt{1-n^2}} \right) \right]}_{\text{dispersion}} \\ & \underbrace{-\nabla h_0}_{\text{potential force}} + \underbrace{\alpha \nabla \left[\frac{1}{1-n^2} \nabla \cdot [(1-n^2)\mathbf{u}] \right]}_{\text{viscous loss}}. \end{aligned} \quad (5b)$$

These equations are an exact transformation of the LL equation. The fluid velocity Eq. (5b) was derived by taking the gradient of the phase or potential equation

$$\begin{aligned} \frac{\partial \Phi}{\partial t} = & -(\sigma - |\mathbf{u}|^2)n + \frac{1}{\sqrt{1-n^2}} \nabla \cdot \left(\frac{\nabla n}{\sqrt{1-n^2}} \right) \\ & + h_0 - \frac{\alpha}{1-n^2} \nabla \cdot [(1-n^2)\mathbf{u}], \end{aligned} \quad (6)$$

which, when $\alpha = 0$, can be interpreted as the magnetic analogue of Bernoulli's equation.

The physical interpretation of each term in Eqs. (5a) and (5b) is specified. Exchange results in long-wave spin density and velocity fluxes in Eqs. (5a) and (5b). These types of long-wave nonlinear effects are well-known in fluid dynamics to give rise to self-steepening and shock formation [32]. Exchange dispersion in Eq. (5b) becomes more pronounced for rapidly varying disturbances, e.g., when self-steepening occurs. The anisotropy factor σ only appears in the velocity flux term in Eq. (5b). Losses are all proportional to α and have intriguing fluid interpretations. For example, the spin relaxation term drives the spin density to the equilibrium configuration $n = h_0/(\sigma - \bar{u}^2)$ [31]. The viscous loss term is the magnetic analogue of viscous friction in a Newtonian fluid.

The first term on the right hand side in Eq. (5a) includes the flux of angular momentum or *spin current density* in the $\hat{\mathbf{z}}$ direction,

$$\mathbf{Q}_s = -\frac{\mu_0 M_s^2 \lambda_{\text{ex}}}{\sqrt{|1 - h_k|}} (1 - n^2) \mathbf{u}, \quad (7)$$

expressed here in units of J/m².

In the context of spin hydrodynamics, Eq. (7) embodies the physical understanding of the fluid variables discussed above. First, the spin density sets the basis direction for the component of spin transport. Second, the prefactor $1 - n^2$ is consistent with the interpretation that a maximal spin current is obtained for saturation, $n = 0$, while no spin current exists at vacuum, $n = \pm 1$. Third, the fluid velocity is directly proportional to the spin current magnitude and describes its flow direction. The same conclusions can be obtained from the point of view of equilibrium spin currents between exchange-coupled spins in a continuum approximation [33].

It is important to stress that the spin current in Eq. (7) is related to hydrodynamic quantities that evolve in time via the DH equations (5a) and (5b). Therefore, the spin current also evolves in time. This feature was recently recognized to describe the far-from-equilibrium transfer of angular momentum in the picosecond evolution of the spatial magnetization in GdFeCo ferrimagnetic amorphous thin films subject to ultrafast optical pumping [34].

3.1.1. Superfluid limit

The DH equations (5a) and (5b) can be simplified in the long wavelength, in-plane limit, when $|n| \ll 1$, $|\mathbf{u}|^2 \ll 1$, $|\nabla n|^2 \ll 1$, and $|\Delta n| \ll 1$. The resulting equations are

$$\frac{\partial n}{\partial t} = \nabla \cdot \mathbf{u} + \alpha \frac{\partial \Phi}{\partial t}, \quad (8a)$$

$$\frac{\partial \mathbf{u}}{\partial t} = \sigma \nabla n - \nabla h_0 + \alpha \nabla (\nabla \cdot \mathbf{u}). \quad (8b)$$

In the idealized scenario of a static texture with constant fluid velocity ($\partial \Phi / \partial t = 0$ and $\nabla \cdot \mathbf{u} = 0$), the damping terms are eliminated from Eqs. (8a) and (8b). This scenario corresponds to the *dissipationless spin transport* identified in Ref. [29]. These equations also support so-called spin superfluids when $\partial \Phi / \partial t \neq 0$ [28]. The analogy between a spin superfluid and superfluid mass transport or charge supercurrent is based on topological arguments: the noncollinear state is mapped into an order parameter that exhibits a nonzero winding number and is formally identical to superfluidity. However, any magnetization dynamics will dissipate energy via damping, as is clear from the viscous terms in Eq. (8b) proportional to α .

3.1.2. Bose-Einstein condensate limit

Another interesting limit is that of a perpendicularly magnetized easy-plane ferromagnet ($\sigma = 1$) subject to small perturbations. In this case, exchange spin waves [35] are excited. The DH equations can be rewritten as a function of the spin density deviation $\rho = 1 - n$, where n is close to 1 (vacuum). The resulting equations, upon renormalization of fluid velocity, space, time, and field read [31]

$$\frac{\partial \rho}{\partial t} + \nabla \cdot (\rho \mathbf{u}) = 0, \quad (9a)$$

$$\frac{\partial \mathbf{u}}{\partial t} + (\mathbf{u} \cdot \nabla) \mathbf{u} + \nabla \rho = \frac{1}{4} \nabla \left[\frac{\Delta \rho}{\rho} - \frac{|\nabla \rho|^2}{2\rho^2} \right] - \nabla h_0, \quad (9b)$$

and describe a repulsive Bose-Einstein condensate (BEC) with trapping potential $U = h_0$ [36]. Physically, this analogy corresponds to the bosonic character of magnons [8].

3.1.3. Two-component Bose-Einstein condensate limit

The conservative, one-dimensional reduction of Eqs. (5a) and (5b), i.e., when $\nabla \rightarrow \partial_x$, $\mathbf{u} = u \cdot \hat{\mathbf{x}}$, and $\alpha = 0$, coincides exactly with the equations describing polarization waves in one-dimensional, two-

component BECs [37, 38]. These equations have been recently shown to support many interesting nonlinear wave phenomena including dispersive shock waves [39] from a fast spatial transition [40, 41].

3.2. Uniform solutions and topology

The simplest solution to Eqs. (5a) and (5b) are the family of static, constant density and fluid velocity states, (\bar{n}, \bar{u}) ,

$$n = \bar{n} = \frac{h_0}{\sigma - \bar{u}^2}, \quad \mathbf{u} = \bar{u}\hat{\boldsymbol{\xi}}, \quad \partial\Phi/\partial t = 0, \quad (10)$$

where $\hat{\boldsymbol{\xi}}$ is the flow direction in the film's plane. These solutions are SDWs that exhibit dissipationless spin transport [29] as described before.

In the conservative limit, when $\alpha = 0$, SDWs can be dynamic, precessional textures. These solutions have been generically termed uniform hydrodynamic states (UHSs) [25, 31] that exhibit a spatially-uniform precessional frequency

$$\partial_t\Phi = \Omega = -(\sigma - \bar{u}^2)\bar{n} + h_0 \quad (11)$$

Both SDWs and UHSs exhibit a single-chirality spatial rotation along the $\hat{\mathbf{z}}$ axis. This implies that both textures are topologically protected via a nonzero winding number [25, 28].

3.3. Spin wave dispersion and stability

The stability of SDWs and UHSs ultimately concerns the manner in which perturbations to these solutions evolve. Generically, small amplitude perturbations are spin waves that carry energy away from the host SDW or UHS. If perturbations grow in time or the generation of spin waves is energetically favorable, then the host state is unstable. This latter rationale was proposed by Landau in his criterion for superfluidity [42] and has been used in the spin superfluid limit [28, 43, 44].

A fluid-centric interpretation of stability criteria can be found by analyzing the spin wave dispersion relation on a UHS background [25, 31]

$$\omega_{\pm}(\mathbf{k}) = 2\bar{n}\bar{u}\hat{\boldsymbol{\xi}} \cdot \mathbf{k} \pm |\mathbf{k}|\sqrt{(1 - \bar{n}^2)(\sigma - \bar{u}^2) + |\mathbf{k}|^2}, \quad (12)$$

where \mathbf{k} is the wave vector. In the long wavelength limit, $|\mathbf{k}| \rightarrow 0$, and if $\hat{\boldsymbol{\xi}} = \mathbf{k}/|\mathbf{k}|$, coincident phase and group velocities allow one to identify the speeds of sound

$$s_{\pm} = 2\bar{n}\bar{u} \pm \sqrt{(1 - \bar{n}^2)(\sigma - \bar{u}^2)}. \quad (13)$$

3.3.1. Modulationally unstable regime

When the speeds in Eq. (13) are *complex*, small fluctuations can grow exponentially. As we now demonstrate, this instability is known as modulational instability (MI) [45, 46].

MI is possible in easy-plane ferromagnets, $\sigma = 1$, only when $|\bar{u}| > 1$. In this case, wavelengths below the exchange length may preclude the validity of the continuum approximation inherent in the LL equation. One potential resolution of such short-wave hydrodynamic effects could lie in a discrete approach [47]. For uniaxial ferromagnets, $\sigma = -1$, the speeds are always complex except when $|\bar{n}| = 1$ (vacuum) so that $\omega_{\pm} = \pm|\mathbf{k}|^2$, i.e., the typical exchange spin wave dispersion relation [35]. In other words, ferromagnets with perpendicular magnetic anisotropy are hydrodynamically unstable and are analogous to attractive BECs [48] and focusing nonlinear optics [49] that support bright solitons. In fact, magnetic solitons in ferromagnets with perpendicular magnetic anisotropy have been predicted and observed [50, 51, 52, 53, 54]. In this case, the exponential growth rate of small perturbations is $\Gamma(k) = \text{Im}\{\omega_{\pm}(k) = \pm k\sqrt{(1 - \bar{n}^2)(\sigma - \bar{u}^2) + k^2}\}$, with $k = |\mathbf{k}|$. Then, the maximum growth rate and associated unstable wavenumber occur when $\Gamma'(k_{\text{max}}) = 0$, given by

$$\Gamma_{\text{max}} = \frac{1}{2}k_c^2, \quad k_{\text{max}} = \frac{1}{\sqrt{2}}k_c, \quad k_c = \sqrt{(1 - \bar{n}^2)(1 - \bar{u}^2)}, \quad (14)$$

where k_c is the cutoff of the unstable band, see Fig. 2. Modulational instability is a long-wavelength instability due to the interaction of nonlinear (PMA) and dispersive (exchange) effects, which are well-known in many physical environments [45, 46].

3.3.2. Modulationally stable regime

For easy-plane ferromagnets, $\sigma = 1$, the speeds of sound in Eq. (13) are always real if $|\bar{u}| \leq 1$. In this case, a scenario similar to the Landau criterion is embodied by the subsonic to supersonic flow transition (when $s_- = 0$ or $s_+ = 0$) quantified by a magnetic Mach number [25]

$$M = |\bar{u}| \sqrt{\frac{1 + 3\bar{n}^2}{1 - \bar{n}^2}}. \quad (15)$$

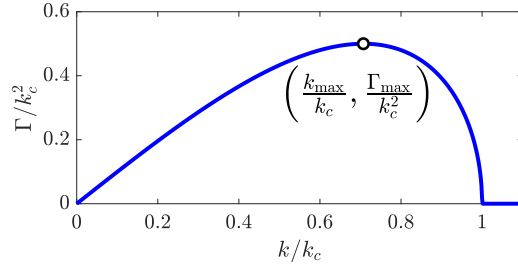


Figure 2: Growth rate of modulationally unstable perturbations. The instability is limited to long waves, with wavevectors below k_c , and exhibits a maximum at the coordinates indicated in Eq. (14).

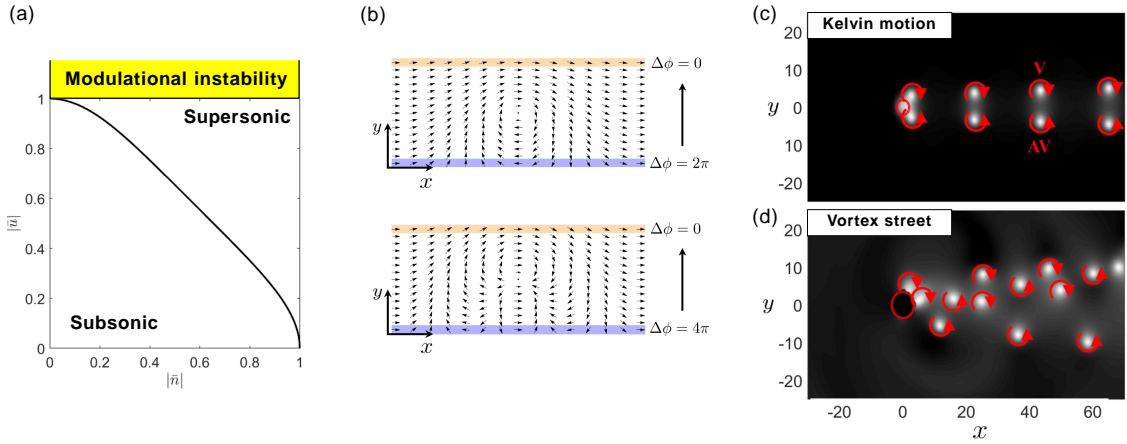


Figure 3: (a) Density vs fluid velocity phase diagram for a UHS in an easy-plane ferromagnet. The solid black curve is the sonic curve where $M = 1$. For $\bar{u} > 1$, UHSs are modulationally unstable. (b) In-plane magnetization component with phase slips mediating a spatial change in the horizontal phase rotations, $\Delta\phi$, of a magnetic texture along the direction y . The top panel shows a transition from a 2π to 0 rotation and the bottom panel a transition from a 4π to 0 rotation. Reprinted figure with permission from S. K. Kim and Y. Tserkovnyak, Phys. Rev. Lett. 116, 127201 (2016). Copyright (2016) by the American Physical Society. Examples of vortex-antivortex shedding from an impenetrable object exhibiting (c) Kelvin motion and (d) a von-Kármán-like vortex street [31]

When $M > 1$, the flow is supersonic and UHSs can be destabilized by a persistent, large-amplitude disturbance, e.g., a physical obstacle [31]. When $M < 1$, the flow is laminar and the UHS stably flows around small obstacles. In the BEC and spin superfluid limits, Eq. (15) is equivalent to the Landau criterion for superfluidity [43]. A density versus fluid velocity sub / supersonic phase diagram is shown in Fig. 3(a).

3.4. Topological defects

Because SDWs and UHSs are topologically protected, instabilities must necessarily lead to the nucleation of topological defects. Chirality can be unwound only through a phase singularity known generically as a phase-slip [28, 55, 56], shown schematically in Fig. 3(b). From a hydrodynamic perspective, such phase-slips are quantized vortices whose core is a density vacuum point, where $n = \pm 1$ [31]. To conserve topology [27],

singularities arise only in pairs whose aggregate topological number is zero, i.e., vortex-antivortex pairs with the same core polarity.

In the presence of finite-sized obstacles, vortex-antivortex pairs can appear even in subsonic conditions. This is because the deflected flow from a physical obstacle can locally become supersonic, resulting in vortex shedding, as is well known for classical fluids undergoing a transition between laminar flow and the onset of turbulence [57, 58]. For easy-plane ferromagnets, such vortex-antivortex pair shedding has been numerically observed [31] as well as their Kelvin motion [59] subject to a texture-induced Magnus force, shown in Fig. 3(c). In addition, the simulations presented in Ref. [31] showed evidence of superfluid-like behavior [60, 61, 62], such as von-Kármán-like vortex streets [63, 64], shown in Fig. 3(d), and Mach cones with radiating wave-fronts ahead of the obstacle [65, 66].

4. Spin transport via spin hydrodynamics

4.1. Boundary value problem

One of the primary motivations to explore spin hydrodynamics in ferromagnets is to beat the exponential decay of spin-wave-mediated spin transport via noncollinear magnetization states. Since typical free spin (open) boundary conditions $\partial\mathbf{m}/\partial\nu = 0$, where ν is the boundary's outward normal, imply $u = 0$, boundary control is needed to sustain noncollinear ($u \neq 0$) spin hydrodynamic states. The simplest example of noncollinear magnetization states have been studied in easy-plane ferromagnetic channels subject to spin injection boundary conditions, shown schematically in Fig 4(a). The boundaries represent magnetic / nonmagnetic interfaces that may be described as perfect spin sources or sinks [67, 68] or imperfect boundaries, e.g., Pt/Py, subject to spin-mixing conductance [69] or spin pumping [70]. Several physical methods for spin injection have been theoretically and experimentally proposed such as the spin-Hall effect [21, 69], spin-transfer torque [67, 68, 70, 71], and the quantum spin-Hall effect [22].

Independent of the theoretical considerations for the boundary conditions, the equilibrium state is a solution to a boundary value problem (BVP). In other words, the solution necessarily spans the length of the channel and the profile of the solution is determined by the particular boundary conditions. This is in stark contrast to spin waves that are solutions to an initial value problem (IVP), i.e., where the

magnet is relaxed into a particular state that is subject to either field or current perturbations and where the transverse physical boundaries play little role in the dominant spin wave characteristics [72]. These fundamental differences between a BVP and an IVP are the reasons why noncollinear magnetization states can beat the exponential decay of spin waves.

For the sake of simplicity, we will consider in this review a perfect spin source coupled with open boundary conditions

$$\frac{\partial n}{\partial x}(t, x = 0) = 0, \quad \frac{\partial n}{\partial x}(t, x = L) = 0, \quad (16a)$$

$$u(t, x = 0) = \bar{u}_0, \quad u(t, x = L) = \bar{u}_L, \quad (16b)$$

where \bar{u}_0 and \bar{u}_L represent fluid velocities at the extrema of a ferromagnetic channel of length L in units of exchange length elongated in the $\hat{\mathbf{x}}$ direction so that the configuration has one-dimensional variation $\mathbf{u}(x) \cdot \hat{\mathbf{x}} = u(x)$.

4.2. Equilibrium solutions

For the case of a channel subject to spin injection on one extremum, $\bar{u}_0 \neq 0$ and $\bar{u}_L = 0$, both linear [28, 69] and nonlinear [25, 68] theory have been used to obtain solutions to the BVP that feature algebraic or near-algebraic spin transport. Furthermore, these equilibrium solutions consist of a coherent, single-frequency precessional state. Because magnetic damping necessarily must be included in the model, solutions to the BVP can be physically interpreted as dynamical modes that persist due to a nonlocal compensation of magnetic damping.

Linear, dispersionless theory based on Eqs. (8a) and (8b) leads to a diffusion equation ultimately resulting in the so-called spin-superfluid [28, 43, 44, 69, 71, 73, 74, 75], alternatively linear dissipative exchange flow (DEF) [68]

$$u(x) = \bar{u}_0 \left(1 - \frac{x}{L}\right), \quad \Omega = -n = \frac{\bar{u}_0}{\alpha L}. \quad (17)$$

This solution is valid for sufficiently weak injection $|\bar{u}_0| \ll \min(1, \alpha L)$. The profile predicted by Eq. (17) is shown in Fig. 4(b) with solid black curves for a ferromagnetic channel of length $L = 100$ and $\alpha = 0.01$ subject to $\bar{u}_0 = 0.2$. The linear solution agrees with the numerically computed solution to the nonlinear

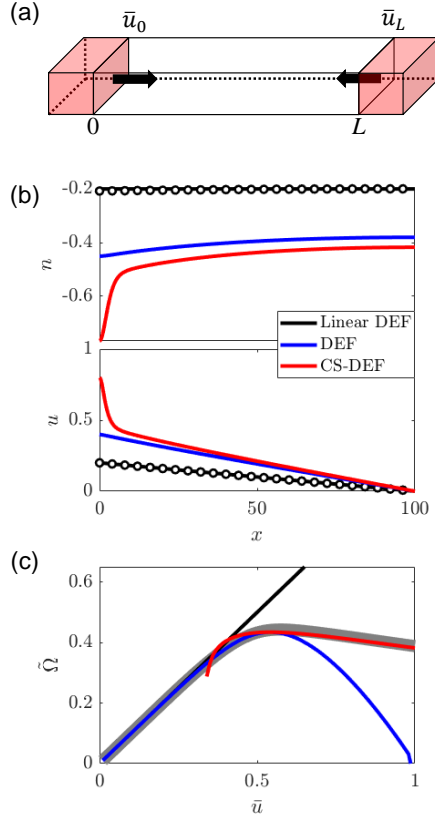


Figure 4: (a) Schematic representation of a ferromagnetic channel subject to spin injection at both extrema. Spin injection can be realized in the red-shaded regions. (b) Density and fluid velocity profiles for the linear analytic solution (black curves) and numerical solution for a linear DEF (black circles), DEF (blue curves), and CS-DEF (red curves) in a ferromagnetic channel of length $L = 100$ and $\alpha = 0.01$. (c) Analytically calculated frequency tunability for each solution. The full numerical solution is shown by a gray curve.

BVP, shown by black circles. For $\bar{u}_0 = 0.4$, the density n exhibits a nonlinear profile as shown by the numerical solution depicted by the solid blue curves. These states have been termed dissipative exchange flows (DEFs) [68]. For even stronger injection, such that the conditions at the injection site are supersonic, a so-called contact soliton centered at $x = 0$ is established, which then matches to a DEF solution. In this case, short-wave exchange dispersion is essential for the existence of a soliton. The numerical solution for this case is shown by the solid red curves when $\bar{u}_0 = 0.8$. The change in the spatial profiles of the solutions is accompanied by a nonlinear frequency tunability that was determined analytically for each case, as shown in Fig. 4(c). The full numerical solution is shown by a gray curve.

Micromagnetic simulations have corroborated the existence of this solution both for ferromagnets [68], termed a contact-soliton DEF, and YIG [70], termed a soliton-screened spin superfluid. Detailed analytical

derivations of all these modes under the DH formulation can be found in Ref. [68].

In the context of spin transport, the fluid velocity is proportional to the spin current, Eq. (7). It is important to recognize that the net spin transport is set by the boundaries. In the ideal case considered here, the net spin transport is zero because there is no spin sink at the right edge. By taking boundaries into account, spin transport is possible [69]. The extreme example is that of a channel where both extrema are subject to spin injection, $\bar{u}_0 \neq 0$ and $\bar{u}_L \neq 0$. In this case, it has been shown that static solutions similar to SDWs can be stabilized in the context of linear theory [76], when $\bar{u}_0 \sim \bar{u}_L$ so that $n = 0$. An analogy to spin Josephson junctions was drawn in Ref. [76], owing to the spatially homogeneous fluid velocity or spin current supported in these states.

Finally, it is worth noting that spin current transport mediated by the precessional frequency of the equilibrium solution is also possible. In this case, the precessional frequency can give rise to a spin current in an adjacent spin reservoir via spin pumping [11, 12].

4.3. *Symmetry-breaking effects*

When the easy-plane symmetry of the system is broken, additional terms that are functions of Φ must be included in Eqs. (5a) and (5b) [67]. This can occur, for example, due to magnetocrystalline anisotropy in soft magnets, nonlocal dipole fields in the LL equation [77], or in-plane applied fields.

For the case of magnetocrystalline anisotropy, the resulting equations of motion take the form of a sine-Gordon equation in the weak-injection regime [28, 67]. Physically, this implies that equilibrium solutions are trains of Néel domain walls with the same chirality. As a consequence, a threshold current exists, proportional to the energy necessary to tilt the magnetization towards the hard axis [28, 67]. The threshold is linearly proportional to the anisotropy field and the channel length for channels shorter than the domain wall width and saturates at a value proportional to the square root of the anisotropy field for long channels [67]. The threshold also induces a reduction in the precessional frequency, reducing the efficiency of spin pumping into a spin reservoir. The predicted threshold spin current density for typical Permalloy material parameters is on the order of 10^{-4} J/m². These values can be obtained by rather large charge current densities on the order of 10^{12} A/m² via spin Hall or spin torque effects. While such charge current densities in principle

achievable, new materials with large spin Hall angle [78] may play an important role to further decrease this figure-of-merit.

Symmetry breaking due to nonlocal dipole fields has been argued to preclude the stabilization of linear DEFs or spin superfluids beyond the distance of an exchange length [73]. However, micromagnetic simulations [25, 67, 68, 70] have demonstrated that SDWs and linear DEF solutions can be stabilized even in the presence of nonlocal dipole fields. Nonlocal dipole has also been studied in the context of the spatial modulation of SDWs [77]. Such a modulation induces a spin wave band diagram, including band gaps, that opens opportunities for noncollinear magnetization states as reprogrammable magnonic crystals [79].

Finally, we remark that finite temperature micromagnetic simulations have also demonstrated the robustness of UHSs and SDWs to stochastic thermal fields [25].

4.4. Other applications

Theoretical studies of current-induced states in ferromagnetic channels have also explored their interactions with other quasi-particles. A temperature gradient along the ferromagnetic channel can excite spin waves [80] that interact with noncollinear magnetization states in a manner described by a two-fluid model composed of a superfluid and normal fluid [75, 81]. It was also shown that thermally activated vortices on a noncollinear magnetization state [56] diffuse along the ferromagnetic channel and can induce a spin current in an adjacent spin reservoir [82].

5. Perspectives and challenges

The field of spin hydrodynamics is undergoing rapid theoretical development that has led to realistic predictions in various contexts. While this review has emphasized ferromagnetic materials, spin hydrodynamics have been extended beyond, including spin transport in antiferromagnets [83, 84], noncollinear antiferromagnets [85], and amorphous materials [86]. These early works have already demonstrated that the hydrodynamic perspective of nonlinear dynamics in magnetic materials results from a distinctly new interpretation that yields significant predictive value. This points toward growing interest in this field of research and a number of intriguing research directions, some of which have already been touched upon in

this review. Examples include the exploration of sub-exchange length hydrodynamics, three-dimensional effects, and the dispersive hydrodynamics of more general magnetic order.

Despite the many theoretical predictions, a conclusive experimental observation of spin hydrodynamics in ferromagnets remains elusive. However, recent experimental evidence in antiferromagnets [21, 22] is promising for the development of experimental spin hydrodynamics in ferromagnets.

Perspectives for spin hydrodynamics may be found by cross-fertilizing with the broader field of fluid dynamics. For example, a hydrodynamic analysis of the spatially varying magnetization of ferrimagnetic GdFeCo subject to ultrafast optical pumping suggests the appearance of localized, topological textures at picosecond timescales as well as the onset of turbulent spin transport [34]. More fundamentally, the role of magnetic damping and its fluid interpretation may lead to additional insights on losses in magnetic texture dynamics. Fruitful future research directions also include time-dependent and emergent phenomena [87] such as rare events e.g., rogue waves [88], and the appearance of nonlinear structures known as dispersive shock waves [39] in both hydrodynamically (modulationally) stable and unstable magnetic configurations. We envision a bright future for the rapidly growing field of spin hydrodynamics.

6. Acknowledgments

E.I. and M.A.H. acknowledge support from the U.S. Department of Energy, Office of Science, Office of Basic Energy Sciences under Award Number DE-SC0017643. M.A.H. partially supported by NSF CAREER DMS-1255422.

References

- [1] D. Sander, S. O. Valenzuela, D. Makarov, C. H. Marrows, E. E. Fullerton, P. Fischer, J. McCord, P. Vavassori, S. Mangin, P. Pirro, B. Hillebrands, A. D. Kent, T. Jungwirth, O. Gutfleisch, C. G. Kim, A. Berger, The 2017 magnetism roadmap, *Journal of Physics D: Applied Physics* 50 (36) (2017) 363001.
- [2] A. Hoffmann, Pure spin-currents, *Phys. Stat. Sol.* 11 (2007) 4236.
- [3] T. Jungwirth, J. Wunderlich, K. Olejník, Spin hall effect devices, *Nature Materials* 11 (2012) 382.
- [4] A. Manchon, H. C. Koo, J. Nitta, S. M. Frolov, R. A. Duine, New perspectives for rashba spin-orbit coupling, *Nature Materials* 14 (2015) 871.
- [5] A. Hoffmann, Spin hall effects in metals, *IEEE Advances on magnetics* 49 (10) (2013) 5172.
- [6] A. M. Humphries, T. Wang, E. R. J. Edwards, S. R. Allen, J. M. Shaw, H. T. Nembach, J. Q. Xiao, T. J. Silva, X. Fan, Observation of spin-orbit effects with spin rotation symmetry, *Nature Communications* 8 (2017) 911.
- [7] M. Kimata, H. Chen, K. Kondory, S. Sugimoto, P. K. Muduli, M. Ikhlas, Y. Omori, T. Tomita, A. H. MacDonald, S. Nakatsuji, T. Otani, Magnetic and magnetic inverse spin hall effects in a non-collinear antiferromagnet, *Nature* 565 (2019) 627.
- [8] R. White, *Quantum theory of magnetism*, Springer, 2007.
- [9] J. C. Slonczewski, Current-driven excitation of magnetic multilayers, *J. Magn. Magn. Mater.* 159 (1-2) (1996) L1 – L7.
- [10] L. Berger, Emission of spin waves by a magnetic multilayer traversed by a current, *Phys. Rev. B* 54 (13) (1996) 9353–9358.

- [11] Y. Tserkovnyak, A. Brataas, G. E. W. Bauer, Enhanced gilbert damping in thin ferromagnetic films, *Phys. Rev. Lett.* 88 (2002) 117601.
- [12] A. Brataas, A. D. Kent, H. Ohno, Current-induced torques in magnetic materials, *Nature Materials* 11 (2012) 372.
- [13] H. Suhl, Theory of the magnetic damping constant, *Magnetics, IEEE Transactions on* 34 (4) (1998) 1834–1838.
- [14] M. Madami, S. Bonetti, G. Consolo, S. Tacchi, G. Carlotti, G. Gubbiotti, F. B. Mancoff, M. A. Yar, J. Åkerman, Direct observation of a propagating spin wave induced by spin-transfer torque, *Nature Nanotechnology* 6 (2011) 635–638.
- [15] T. L. Gilbert, A phenomenological theory of damping in ferromagnetic materials, *Magnetics, IEEE Transactions on* 40 (6) (2004) 3443 – 3449.
- [16] A. V. Chumak, V. I. Vasyuchka, A. A. Serga, B. Hillebrands, Magnon spintronics, *Nature physics* 11 (2015) 453.
- [17] L. J. Cornelissen, J. Liu, R. A. Duine, J. B. Youssef, B. J. van Wees, Long-distance transport of magnon spin information in a magnetic insulator at room temperature, *Nature Physics* 11 (2015) 1022.
- [18] C. Liu, J. Chen, T. Liu, F. Heimbach, H. Yu, Y. Xiao, J. Hu, M. Liu, H. Chang, T. Stueckler, S. tu, Y. Zhang, Y. Zhang, P. Gao, Z. Liao, D. Yu, K. Xia, N. Lei, W. Zhao, M. Wu, Long-distance propagation of short-wavelength spin waves, *Nature Communications* 9 (2018) 738.
- [19] D. Wesenberg, T. Liu, D. Balzar, M. Wu, B. L. Zink, Long-distance spin transport in a disordered magnetic insulator, *Nature Physics* 13 (2017) 987.
- [20] R. Lebrun, A. Ross, S. A. Bender, A. Qaiumzadeh, L. Baldrati, J. Cramer, A. Brataas, R. A. Duine, M. Kläui, Tunable long-distance spin transport in crystalline antiferromagnetic iron oxide, *Nature Physics* 561 (2018) 222.
- [21] P. Stepanov, S. Che, D. Shcherbakov, J. Yang, R. Chen, K. Thilagar, G. Voigt, M. W. Bockrath, D. Smirnov, K. Watanabe, T. Taniguchi, R. K. Lake, Y. Barlas, A. H. MacDonald, C. N. Lau, Long-distance spin transport through a graphene quantum hall antiferromagnet, *Nature Physics* 14 (2018) 907.
- [22] W. Yuan, Q. Zhu, T. Su, Y. Yao, W. Xing, Y. Chen, Y. Ma, X. Lin, J. Shi, R. Shindou, X. C. Xie, W. Han, Experimental signatures of spin superfluid ground state in canted antiferromagnet Cr_2O_3 via nonlocal spin transport, *Science Advances* 4 (2018) eaat1098.
- [23] L. D. Landau, E. Lifshitz, On the theory of the dispersion of magnetic permeability in ferromagnetic bodies, *Phys. Z. Sowjet.* 8 (1953) 153.
- [24] P. Bruno, J. P. Renard, Magnetic surface anisotropy of transition metal ultrathin films, *Applied Physics A: Materials Science & Processing* 49 (1989) 499–506, 10.1007/BF00617016.
- [25] E. Iacocca, T. J. Silva, M. A. Hofer, Breaking of galilean invariance in the hydrodynamic formulation of ferromagnetic thin films, *Phys. Rev. Lett.* 118 (2017) 017203.
- [26] B. Halperin, P. Hohenberg, Hydrodynamic theory of spin waves, *Physical Review* 188 (2) (1969) 898–918.
- [27] N. Papanicolaou, T. Tomaras, Dynamics of magnetic vortices, *Nuclear Physics B* 360 (2-3) (1991) 425–462.
- [28] E. B. Sonin, Spin currents and spin superfluidity, *Advances in Physics* 59 (3) (2010) 181 – 255.
- [29] J. König, M. C. Bønsager, A. H. MacDonald, Dissipationless spin transport in thin film ferromagnets, *Phys. Rev. Lett.* 87 (2001) 187202.
- [30] G. Grüner, The dynamics of spin-density waves, *Rev. Mod. Phys.* 66 (1994) 1–24.
- [31] E. Iacocca, M. A. Hofer, Vortex-antivortex proliferation from an obstacle in thin film ferromagnets, *Phys. Rev. B* 95 (2017) 134409.
- [32] L. D. Landau, E. M. Lifshitz, *Fluid Mechanics*, Pergamon press, 1987.
- [33] P. Bruno, V. K. Dugaev, Equilibrium spin currents and the magnetoelectric effect in magnetic nanostructures, *Phys. Rev. B* 72 (2005) 241302.
- [34] E. Iacocca, T.-M. Liu, A. H. Reid, Z. Fu, S. Ruta, P. W. Granitzka, E. Jal, S. Bonetti, A. X. Gray, C. E. Graves, R. Kukreja, Z. Chen, D. J. Higley, T. Chase, L. Le Guyader, K. Hirsch, H. Ohldag, W. F. Schlotter, G. L. Dakovski, G. Coslovich, M. C. Hoffmann, S. Carron, A. Tsukamoto, A. Kirilyuk, A. V. Kimel, T. Rasing, J. Stöhr, R. F. L. Evans, T. Ostler, R. W. Chantrell, M. A. Hofer, T. J. Silva, , H. A. Dürr, Spin-current-mediated rapid magnon localization and coalescence after ultrafast optical pumping of ferrimagnetic alloys, *Nature Communications* 10 (2019) 1756.
- [35] D. Stancil, A. Prabhakar, *Spin waves: Theory and applications*, Springer, 2009.
- [36] C. Pethick, H. Smith, *Bose-Einstein condensation in dilute gasses*, Cambridge University Press, 2002.
- [37] C. Qu, L. P. Pitaevskii, S. Stringari, Magnetic solitons in a binary bose-einstein condensate, *Phys. Rev. Lett.* 116 (2016) 160402.
- [38] T. Congy, A. M. Kamchatnov, N. Pavloff, Dispersive hydrodynamics of nonlinear polarization waves in two-component Bose-Einstein condensates, *SciPost Phys.* 1 (2016) 006.
- [39] G. El, M. Hofer, Dispersive shock waves and modulation theory, *Physica D*, to appear.
- [40] S. K. Ivanov, A. M. Kamchatnov, T. Congy, N. Pavloff, Solution of the riemann problem for polarization waves in a two-component bose-einstein condensate, *Phys. Rev. E* 96 (2017) 062202.
- [41] S. K. Ivanov, A. M. Kamchatnov, Simple waves in a two-component bose-einstein condensate, *Phys. Rev. E* 97 (2018) 042208.
- [42] L. D. Landau, Theory of the superfluidity of helium II, *J. Phys. USSR* 5 (1941) 71.
- [43] E. B. Sonin, Spin superfluidity and spin waves in yig films, *Phys. Rev. B* 95 (2017) 144432.
- [44] E. B. Sonin, Superfluid spin transport in ferro- and antiferromagnets, *Phys. Rev. B* 99 (2019) 104423.
- [45] G. B. Whitham, *Linear and nonlinear waves*, John Wiley & Sons Inc, 1974.
- [46] V. Zakharov, L. Ostrovsky, Modulation instability: The beginning, *Physica D* 238 (2009) 540–548.
- [47] R. F. L. Evans, W. J. Fan, P. Chureemart, T. A. Ostler, M. A. A. Allis, R. W. Chantrell, Atomistic spin model simulations of magnetic nanomaterials, *J. Phys.: Condens. Matter* 26 (2014) 103202.
- [48] P. G. Kevrekidis, D. J. Frantzeskakis, R. Carretero-González, *The Defocusing Nonlinear Schrödinger Equation*, SIAM,

Philadelphia, 2015.

- [49] Y. Kivshar, G. Agrawal, Optical solitons, Elsevier, 2003.
- [50] A. Kosevich, B. Ivanov, A. Kovalev, Magnetic solitons, Physics Reports 194 (3–4) (1990) 117 – 238.
- [51] M. A. Hoefer, T. J. Silva, M. W. Keller, Theory for a dissipative droplet soliton excited by a spin torque nanocontact, Phys. Rev. B 82 (2010) 054432.
- [52] S. M. Mohseni, S. R. Sani, J. Persson, T. N. A. Nguyen, S. Chung, Y. Pogoryelov, P. K. Muduli, E. Iacocca, A. Eklund, R. K. Dumas, S. Bonetti, A. Deac, M. A. Hoefer, J. Åkerman, Spin torque-generated magnetic droplet solitons, Science 339 (6125) (2013) 1295–1298.
- [53] D. Backes, F. Macià, S. Bonetti, R. Kukreja, H. Ohldag, A. D. Kent, Direct observation of a localized magnetic soliton in a spin-transfer nanocontact, Phys. Rev. Lett. 115 (2015) 127205.
- [54] S. Chung, Q. T. Le, M. Ahlberg, A. A. Awad, M. Weigand, I. Bykova, R. Khymyn, M. Dvornik, H. Mazraati, A. Houshang, S. Jiang, T. N. A. Nguyen, E. Goering, G. Schütz, J. Gräfe, J. Åkerman, Direct observation of zhang-li torque expansion of magnetic droplet solitons, Phys. Rev. Lett. 120 (2018) 217204.
- [55] S. K. Kim, Y. Tserkovnyak, Topological effects on quantum phase slips in superfluid spin transport, Phys. Rev. Lett. 116 (2016) 127201.
- [56] S. K. Kim, S. Takei, Y. Tserkovnyak, Thermally activated phase slips in superfluid spin transport in magnetic wires, Phys. Rev. B 93 (2016) 020402.
- [57] C. H. K. Williamson, Vortex Dynamics in the Cylinder Wake, Annual Review of Fluid Mechanics 28 (1) (1996) 477–539.
- [58] T. Leweke, S. Le Dizès, C. H. K. Williamson, Dynamics and instabilities of vortex pairs, Annual reviews of Fluid Mechanics 48 (2016) 506–541.
- [59] N. Papanicolaou, P. N. Spathis, Semitopological solitons in planar ferromagnets, Nonlinearity 12 (1999) 285.
- [60] M. T. Reeves, T. P. Billam, B. P. Anderson, A. S. Bradley, Identifying a superfluid reynolds number via dynamical similarity, Phys. Rev. Lett. 114 (2015) 155302.
- [61] T. Frisch, Y. Pomeau, S. Rica, Transition to dissipation in a model of superflow, Phys. Rev. Lett. 69 (1992) 1644–1647.
- [62] C. Nore, M. Brachet, S. Fauve, Numerical study of hydrodynamics using the nonlinear schrödinger equation, Physica D: Nonlinear Phenomena 65 (1) (1993) 154 – 162.
- [63] K. Sasaki, N. Suzuki, H. Saito, Bénard–von kármán vortex street in a bose-einstein condensate, Phys. Rev. Lett. 104 (2010) 150404.
- [64] W. J. Kwon, J. H. Kim, S. W. Seo, Y. Shin, Observation of von kármán vortex street in an atomic superfluid gas, Phys. Rev. Lett. 117 (2016) 245301.
- [65] I. Carusotto, S. X. Hu, L. A. Collins, A. Smerzi, Bogoliubov–Čerenkov radiation in a bose-einstein condensate flowing against an obstacle, Phys. Rev. Lett. 97 (2006) 260403.
- [66] Y. G. Gladush, G. A. El, A. Gammal, A. M. Kamchatnov, Radiation of linear waves in the stationary flow of a bose-einstein condensate past an obstacle, Phys. Rev. A 75 (2007) 033619.
- [67] E. Iacocca, T. J. Silva, M. A. Hoefer, Symmetry-broken dissipative exchange flows in thin-film ferromagnets with in-plane anisotropy, Phys. Rev. B 96 (2017) 134434.
- [68] E. Iacocca, M. A. Hoefer, Hydrodynamic description of long-distance spin transport through noncollinear magnetization states: Role of dispersion, nonlinearity, and damping, Phys. Rev. B 99 (2019) 184402.
- [69] S. Takei, Y. Tserkovnyak, Superfluid spin transport through easy-plane ferromagnetic insulators, Phys. Rev. Lett. 112 (2014) 227201.
- [70] T. Schneider, D. Hill, A. Kákay, K. Lenz, J. Lindner, J. Fassbender, P. Upadhyaya, Y. Liu, K. Wang, Y. Tserkovnyak, I. N. Krivorotov, I. Barsukov, Self-stabilizing spin superfluid, arXiv:1811.09369.
- [71] H. Chen, A. D. Kent, A. H. MacDonald, I. Sodemann, Nonlocal transport mediated by spin supercurrents, Phys. Rev. B 90 (2014) 220401.
- [72] T. Chen, R. K. Dumas, A. Eklund, P. K. Muduli, A. Houshang, A. A. Awad, P. Dürrenfeld, B. G. Malm, A. Rusu, J. Åkerman, Spin-torque and spin-hall nano-oscillators, Proceedings of the IEEE 104 (10) (2016) 1919–1945.
- [73] H. Skarsvåg, C. Holmqvist, A. Brataas, Spin superfluidity and long-range transport in thin-film ferromagnets, Phys. Rev. Lett. 115 (2015) 237201.
- [74] S. Takei, Y. Tserkovnyak, Nonlocal magnetoresistance mediated by spin superfluidity, Phys. Rev. Lett. 115 (2015) 156604.
- [75] B. Flebus, S. A. Bender, Y. Tserkovnyak, R. A. Duine, Two-fluid theory for spin superfluidity in magnetic insulators, Phys. Rev. Lett. 116 (2016) 117201.
- [76] D. Hill, S. K. Kim, Y. Tserkovnyak, Spin-torque-biased magnetic strip: Nonequilibrium phase diagram and relation to long josephson junctions, Phys. Rev. Lett. 121 (2018) 037202.
- [77] P. Sprenger, M. A. Hoefer, E. Iacocca, Magnonic band structure established by chiral spin-density waves in thin-film ferromagnets, IEEE Magnetics Letters 10 (2019) 4501605.
- [78] M. W. Keller, K. S. Gerace, M. Arora, E. K. Delczeg-Czirjak, J. M. Shaw, T. J. Silva, Near-unity spin hall ratio in Ni_xCu_{1-x} alloys, Phys. Rev. B 99 (2019) 214411.
- [79] M. Krawczyk, D. Grundler, Review and prospects of magnonic crystals and devices with reprogrammable band structure, Journal of Physics: Condensed Matter 26 (12) (2014) 123202.
- [80] K. Uchida, S. Takahashi, K. Harii, J. Ieda, W. Koshibae, K. Ando, S. Maekawa, E. Saitoh, Observation of the spin seebeck effect, Nature 455 (2008) 778.
- [81] Y. Tserkovnyak, S. A. Bender, R. A. Duine, B. Flebus, Bose-einstein condensation of magnons pumped by the bulk spin seebeck effect, Phys. Rev. B 93 (2016) 100402.
- [82] S. K. Kim, S. Takei, Y. Tserkovnyak, Topological spin transport by brownian diffusion of domain walls, Phys. Rev. B 92 (2015) 220409.

- [83] S. Takei, B. I. Halperin, A. Yacoby, Y. Tserkovnyak, Superfluid spin transport through antiferromagnetic insulators, *Phys. Rev. B* 90 (2014) 094408.
- [84] A. Qaiumzadeh, H. Skarsvåg, C. Holmqvist, A. Brataas, Spin superfluidity in biaxial antiferromagnetic insulators, *Phys. Rev. Lett.* 118 (2017) 137201.
- [85] J. S. Y. Yamane, O. Gomonay, Dynamics of noncollinear antiferromagnetic textures driven by spin current injection, arXiv:1901.05684.
- [86] H. Ochoa, R. Zarzuela, Y. Tserkovnyak, Spin hydrodynamics in amorphous magnets, *Phys. Rev. B* 98 (2018) 054424.
- [87] M. Buzzi, M. Först, R. Mankowsky, A. Cavalleri, Probing dynamics in quantum materials with femtosecond x-rays, *Nature Reviews Materials* 3 (2018) 299.
- [88] A. Chabchoub, M. Onorato, N. Akhmediev, *Hydrodynamic envelope solitons and breathers*, Springer, 2016, Ch. 3, pp. 55–87.